

# Combining Ink-Jet Printing with Emulsion Solvent-Evaporation to Pattern Polymeric Particles

*Renhua Deng, Lisong Yang, and Colin D. Bain\**

Department of Chemistry, Durham University, Stockton Road, Durham DH1 3LE, U.K.

KEYWORDS: ink-jet printing, polymers, emulsion, polymeric particles

ABSTRACT: We demonstrate a concept to produce deposits of polymer in the form of particles by ink-jet printing an emulsion in which the discrete phase evaporates preferentially. An oil/water emulsion with polymer contained inside the oil phase is used as ink for printing. Flat deposits of spherical polymer particles with uniform thickness are obtained. The effects of the hydrophobicity of substrates and the physical properties of the oil on the morphology of the deposits are explored. The deposit of aggregated polymeric particles can be transformed into a uniform film by annealing if required. This strategy for patterning of polymer materials in the form of either particles or film works for mixtures of polymers and functional cargoes.

Ink-jet printing possesses attractive features as a manufacturing technology including efficient use of materials, digital control over patterns, flexible substrates and a contact-free process.<sup>1-6</sup> Increasing attention is being paid to ink-jet printing of polymers because of emerging applications beyond conventional graphics, such as conducting polymeric devices, organic solar cells and organic light-emitting diodes.<sup>7-12</sup> However, polymer solutions with relatively high concentrations (> 1 wt.%) become difficult to print reliably owing to viscoelasticity of the polymer solution, especially for high-molecular-weight polymers.<sup>13,14</sup> Johns and Bain recently overcame this problem by confining the polymers within the oleic phase of an oil-in-water (O/W) emulsion.<sup>15</sup> These inks exhibit low viscosity even at high polymer concentrations. Shear occurs exclusively in the continuous aqueous phase so that the viscoelasticity of the polymer-containing phase does not inhibit the ejection of droplets or the break-up of ligaments. In the experiments of Johns and Bain, the oil was less volatile than water and the oil droplets coalesced during evaporation leading to a polymeric film upon subsequent evaporation of the oil.

Pre-formed polymer particles can be printed as a colloidal dispersion to yield structured deposits with potential applications as photonic crystals.<sup>16-20</sup> Uniform deposits with an ordered structure are desired in most applications. In practice, ring stains commonly arise due to radial capillary flow in the drops during evaporation which deposits particles at the periphery of the drop (widely known as the coffee-ring effect (CRE)). The CRE is particularly pronounced for pinned contact lines and contact angles of less than 90°. <sup>21-24</sup> Many approaches have been taken to weaken the radial capillary flow in order to inhibit formation of ring stains including the use of mixtures of volatile solvents, external fields to induce particle motion, or interactions among particles or between the particles and the solvent.<sup>25-32</sup> For example, Talbot and Bain utilized an evaporation-driven sol-gel transition in laponite suspensions to suppress the radial capillary flow and obtain uniform deposits

of polymer nanospheres.<sup>33</sup> Previous inkjet studies aimed at depositing polymeric particles invariably used colloidal dispersions of pre-formed particles. However, the commercial availability of particles – especially functional particles – is limited and they are expensive relative to the constituent bulk polymers. Emulsion solvent-evaporation is a versatile method for preparation of polymer particles. In this method, the discrete phase is chosen to be more volatile than the continuous phase so that preferential evaporation of the droplets generates particles rather than a continuous film of polymer. Deng and co-workers have shown how the size, shape and structure of polymeric particles can be controlled.<sup>34-36</sup>

In this study, we have combined ink-jet printing with emulsion solvent-evaporation to produce deposits of polymeric particles directly. An O/W emulsion with polymer contained in the high-density oil phase is used as ink for printing. Disk-shaped deposits with uniform thickness and a low height/diameter ratio are achievable by this strategy. In addition, the deposit of aggregated polymeric particles can be transformed into a film upon annealing if required. Patterns are repeatable from polymers with various molecular weight and chemical compositions, which is essential for practical applications.

Polystyrene (PS<sub>35K</sub>,  $M_w = 35 \text{ kg mol}^{-1}$ ) dissolved in a volatile water-immiscible solvent, dichloromethane (DCM), was used as the oil phase and dispersed in an aqueous solution of the surfactant sodium dodecyl sulfate (SDS). These two solutions were homogenized to produce an O/W emulsion (see Supporting Information for experimental detail). The emulsion had most oil droplets below 10  $\mu\text{m}$  in diameter (Figure 1a) and were printed through a print head (Microfab) with a 50- $\mu\text{m}$  diameter orifice onto a transparent hydrophobic substrate (water contact angle,  $\theta_{\text{H}_2\text{O}} = 88 \pm 3^\circ$ ). The evaporation process was recorded through the substrate (Video S1). Figure 1b shows a set of still images extracted from the video to show the three stages of evaporation

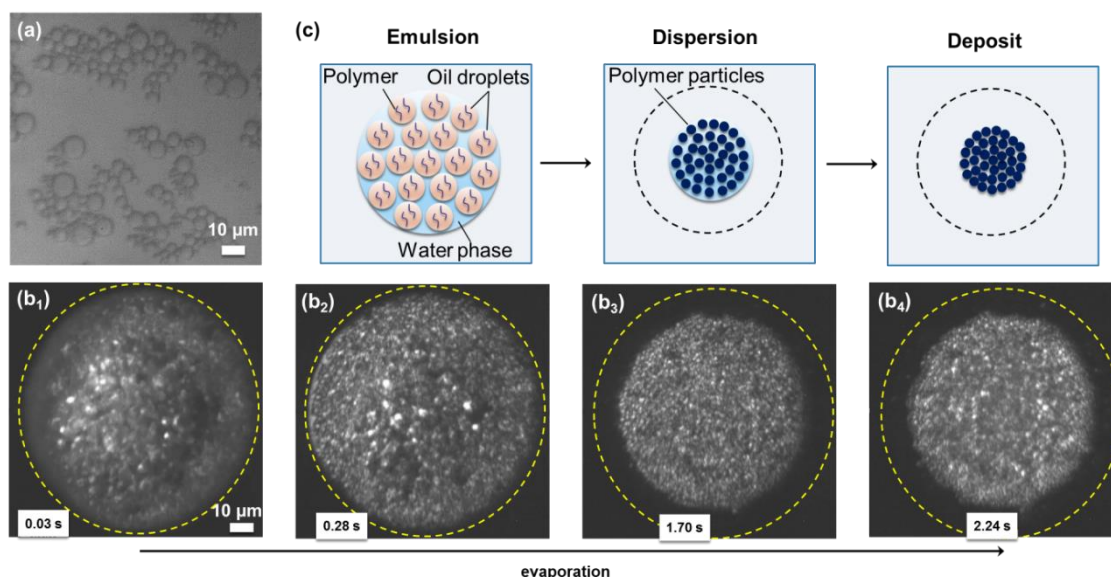


**Figure 1.** Ink-jet printing of O/W emulsion (O: 10.0 mg/mL PS/DCM; W: 3.0 mg/mL SDS/water; volume ratio O/W = 1/3). (a) Bright-field micrograph of the emulsion; (b<sub>1</sub> – b<sub>4</sub>) dark-field micrographs of the evolution of an ejected emulsion drop on the substrate during evaporation, (b<sub>1</sub>) 0.03 s, (b<sub>2</sub>) 0.28 s, (b<sub>3</sub>) 1.70 s, and (b<sub>4</sub>) 2.24 s; (c) schematic diagrams showing the evolution of a printed drop. The dashed yellow line indicates the position of the contact line after the initial impact and spreading of the droplet.

and deposition. During stage 1 (0.03–0.28 s), oil droplets spread towards to the contact line (Figure 1b<sub>1</sub> and 1b<sub>2</sub>). During stage 2 (0.28–1.70 s), the reverse (inward) motion of the oil droplets (or formed particles) from the edge back towards the centre was observed (Figure 1b<sub>3</sub>), possibly due to capillary forces near the contact line.<sup>37</sup> During stages 1 and 2, the drop underwent an emulsion-to-dispersion transition: most oil droplets had evaporated (DCM diffuses through the water and then evaporates from air/water interface) and formed particles, while the continuous aqueous phase (water) had not dried fully. In stage 3 (1.70–2.24 s), complete evaporation of the continuous phase of the dispersion resulted in the formation of a circular deposit with size (~85 μm) slightly smaller

than initial contact line (Figure 1b<sub>4</sub>). No ring stain was observed. Figure 2 shows the evaporation process schematically together with corresponding images acquired from the side. The droplet remains as a spherical cap with pinned contact line until the final stages of evaporation.

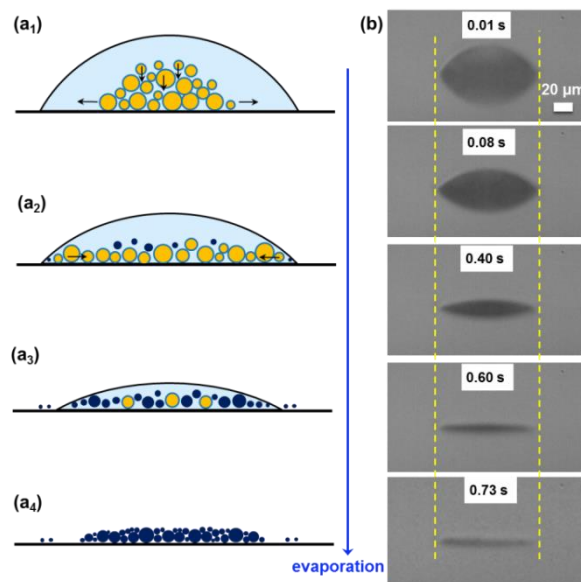


**Figure 2.** (a) Schematic diagrams and (b) micrographs showing the evaporation of a printed drop of emulsion viewed from the side. The reflection of the drop in the substrate is also seen.

The morphology of the deposit was investigated by scanning electron microscopy (SEM) and atomic force microscopy (AFM) (Figure 3 and Figure S1). The polymer particles are spherical and polydisperse with diameters from submicron to  $\sim 2.8$  microns. The size distribution is determined by the initial droplet size distribution in the O/W emulsion and the polymer concentration. In the SEM image at higher magnification (Figure 3a<sub>2</sub>), a few small nanoparticles are observed close to the contact line, probably because capillary forces drive larger particles away from the contact line.<sup>37</sup> The AFM analysis (Figure 3b<sub>1</sub> and 3b<sub>2</sub>) indicates that the thickness of the deposit is uniform on a length scale much larger than individual particles, with a height of  $\sim 2.6$   $\mu\text{m}$  (see the cross section in Figure 3c). Flat deposits without ring stains are desired in most applications, such as

graphics printing and printed electronics. In previous studies, hydrophobic substrates ( $\theta_{H_2O} > 90^\circ$ ) have usually been adopted in order to avoid the CRE; however, a receding contact line usually then gives hemi-spherical deposits of colloidal particles.<sup>17,19,31</sup> The uniform deposit obtained on hydrophobic substrate by our method can be explained by several factors: 1) the presence of a surfactant greatly reduces the initial contact angle<sup>38</sup> of the ink after spreading (Figure 2b); 2) the evaporative model<sup>39</sup> of the emulsion is a constant contact area mode with a decreasing contact angle (Figure 2b and Video S2), different from that of water (Figure S2) on the same substrate; 3) the oil droplets tend to settle under gravity due to the high density of the solvent ( $\rho_{DCM} = 1.33 \text{ g cm}^{-3}$ ); 4) the layer of oil droplets suppresses radial capillary flow near the substrate.

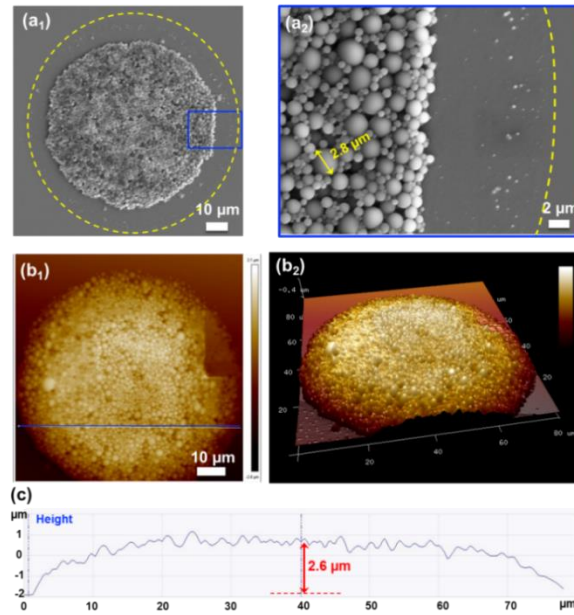


**Figure 3.** (a<sub>1</sub> and a<sub>2</sub>) SEM images of the deposit from a printed emulsion drop; (b<sub>1</sub>) 2D and (b<sub>2</sub>) 3D AFM images of the deposit, and (c) a height curve of the cross-section along the blue line in (b<sub>1</sub>).

The morphology of deposits in ink-jet printing is well known to depend strongly on the

wettability of the ink on the substrate<sup>40-43</sup>. Substrates with varying hydrophobicity were prepared by chemical modification with different silanes, and the corresponding deposits from printed emulsions are shown in Figure S3. This group of results indicate that 1) the wettability of the emulsion is less sensitive to the nature of the substrates than that of water mainly due to the presence of surfactant; 2) the diameter of deposits increases with the decrease of contact angle as would be expected from volume conservation; 3) irregular deposits formed on either strongly hydrophobic ( $\theta_{\text{H}_2\text{O}} = 107^\circ$ ) or strongly hydrophilic ( $\theta_{\text{H}_2\text{O}} = 20^\circ$ ) substrates; and 4) uniform deposits are repeatable on substrates with  $\theta_{\text{H}_2\text{O}}$  in the range of  $\sim 60^\circ$ – $90^\circ$ , which is an important feature for future applications.

The choice of non-polar solvent was also explored. In addition to low solubility in water, the oleic solvents must evaporate faster than water in order to generate polymeric particles. When a solvent (such as methyl benzoate) is used that evaporates more slowly than water, an emulsion-to-solution transition occurs and the deposit is in the form of a film (Figure S4a) rather than particles. Ethyl acetate is more volatile than water but, in contrast to DCM, has a lower density than water. In this case, the oil droplets rise towards the top of the emulsion and some coalescence of droplets occurred resulting in the generation of larger particles (Figure S4b). The CRE was observed in the deposit, due to the radial capillary flow during evaporation (Video S3). We infer that the relative density of the solvent plays a role in the morphology of deposits. Uniform deposit of polymer particles was observed (Figure S4c) with chloroform, another volatile and high-density solvent similar to DCM.

Inkjet printing of polymeric inks becomes increasingly problematic as the molecular weight increases.<sup>14</sup> To explore the sensitivity of our method to molecular weight we repeated the experiments in Figure 1 with PS with a molecular weight of  $253 \text{ kg mol}^{-1}$ . A deposit similar to

that of PS<sub>35K</sub> was obtained (Figure 4a). We also studied emulsions of PS<sub>35K</sub> with a higher concentration of polymer in the oleic phase: 50 mg mL<sup>-1</sup> (Figure 4b). The method can be extended to other water-insoluble polymers: Figure 4c shows a deposit of PMMA particles formed in situ by printing of an emulsion. Functional species can be loaded inside the polymeric particles during printing. A model cargo, Nile Red, was mixed with PS at a mass ratio of 1:100 before printing. Encapsulation of Nile Red is confirmed by fluorescence spectroscopy (Figure 4d<sub>2</sub> and d<sub>3</sub>). Moreover, the emulsion formulation also permits the production of particles loaded with functional species such as drugs, magnetic nanoparticles or quantum dots,<sup>44</sup> providing a method for creation of which would be worth considering for functional patterns by ink-jet printing.

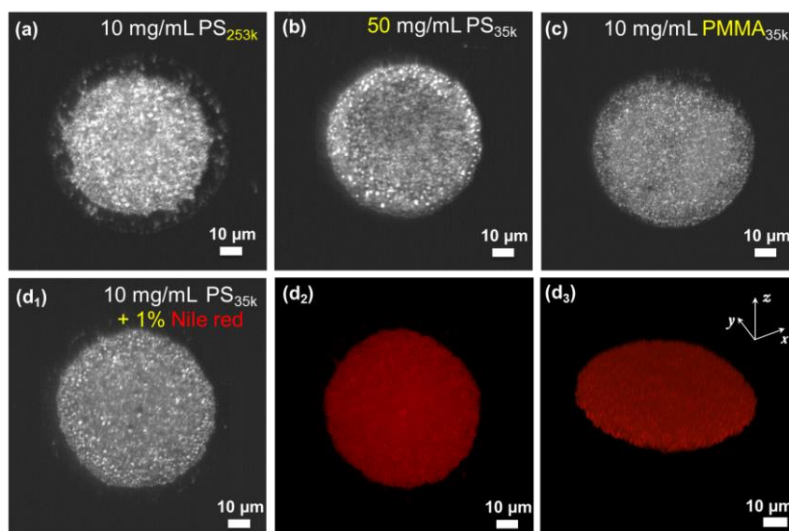


**Figure 4.** Dark field micrographs of deposits from polymers with varied molecular weight (a), concentration (b) and composition (c and d<sub>1</sub>); (d<sub>2</sub>) 2D and (d<sub>3</sub>) 3D reconstruction super resolution fluorescence spectroscopy<sup>45</sup> images of the deposit in (d<sub>1</sub>).

The particles formed in this study are polydisperse and therefore of little use for applications in photonics. Future work will explore the production of monodisperse particles by inkjet printing of



oil droplets of uniform size. On the other hand, the deposits of polymeric particles can be transformed into films by annealing. Upon heating above the glass transition temperature,  $T_g$ , of the polymer, the particles melt and coalesce into a film, as shown in Figure 5. The film adopted the footprint of the precursor deposit of particles. The film obtained by the current method is more regular in shape and uniform in thickness than the film obtained directly by printing of an emulsion with methyl benzoate as the solvent of the oil phase (Figure S4a).

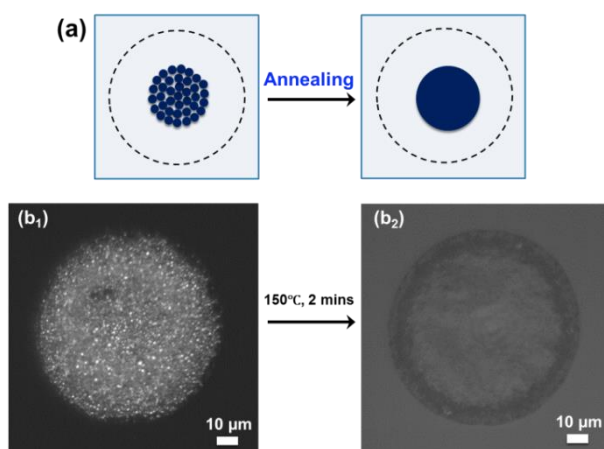


**Figure 5.** (a) Schematic diagram showing transformation of the deposit by annealing: (b<sub>1</sub>) dark field micrograph of a deposit before annealing, and (b<sub>2</sub>) bright field micrograph of the deposit after annealing.

In summary, we have presented a method to obtain deposits of polymers in the form of particles via ink-jet printing of emulsions. Polymeric particles formed in-situ in the drying droplet through the prior evaporation of the dispersed phase solvent. Disk-shaped deposits with uniform thickness and a size slightly smaller than contact line can be generated in seconds. The morphology of the deposits is dependent on the wetting properties of substrate and the nature of the oil solvent. Functional cargoes can be encapsulated inside the polymeric particles during printing. Deposits of

polymeric particles can easily be transformed into films by annealing if required. In principle, this method is versatile for depositing particles formed from a wide range of water-insoluble species and their mixtures.

## ASSOCIATED CONTENT

### **Supporting Information.**

Experimental Section, additional figures and video. The following files are available free of charge via the Internet at <http://pubs.acs.org>.

Experimental Section and additional figures (PDF)

Videos of the evaporation of printed drops (AVI)

## AUTHOR INFORMATION

### **Corresponding Author**

\*E-mail: [c.d.bain@durham.ac.uk](mailto:c.d.bain@durham.ac.uk)

### **Notes**

The authors declare no competing financial interest.

## ACKNOWLEDGMENT

The authors are grateful to Axa A. Pineiro-Romero for SEM imaging and Dr. Robert Pal for fluorescence microscopy imaging. This work was funded by EPSRC under Grant EP/N025245/1.

## REFERENCES

- (1) Singh, M.; Haverinen, H. M.; Dhagat, P.; Jabbour, G. E. Inkjet Printing-Process and Its Applications. *Adv. Mater.* **2010**, *22*, 673-685.
- (2) Le, H. P. Progress and Trends in Ink-Jet Printing Technology. *J. Imag. Sci. Technol.* **1998**, *42*, 49-62.
- (3) Park, J.-U.; Hardy, M.; Kang, S. J.; Barton, K.; Adair, K.; Mukhopadhyay, D. k.; Lee, C. Y.; Strano, M. S.; Alleyne, A. G.; Georgiadis, J. G.; Ferreira, P. M.; Rogers, J. A. High-Resolution Electrohydrodynamic Jet Printing. *Nature Mater.* **2007**, *6*, 782-789.
- (4) Calvert, P. Inkjet Printing for Materials and Devices. *Chem. Mater.* **2001**, *13*, 3299-3305.
- (5) Gillen, G.; Najarro, M.; Wight, S.; Walker, M.; Verkouteren, J.; Windsor, E.; Barr, T.; Staymates, M.; Urbas, A. Particle Fabrication Using Inkjet Printing onto Hydrophobic Surfaces for Optimization and Calibration of Trace Contraband Detection Sensors. *Sensors* **2015**, *15*, 29618-29634.
- (6) Fletcher, R. A.; Brazin, J. A.; Staymates, M. E.; Benner, B. A.; Gillen, J. G. Fabrication of Polymer Microsphere Particle Standards Containing Trace Explosives Using an Oil/Water Emulsion Solvent Extraction Piezoelectric Printing Process. *Talanta* **2008**, *76*, 949-955.
- (7) Spinelli, H. J. Polymeric Dispersants in Ink Jet Technology. *Adv. Mater.* **1998**, *10*, 1215-1218.
- (8) Sirringhaus, H.; Kawase, T.; Friend, R. H.; Shimoda, T.; Inbasekaran, M.; Wu, W.; Woo, E. P. High-Resolution Inkjet Printing of All-Polymer Transistor Circuits. *Science* **2000**, *290*, 2123-2126.
- (9) de Gans, B. J.; Duineveld, P. C.; Schubert, U. S. Inkjet Printing of Polymers: State of the Art and Future Developments. *Adv. Mater.* **2004**, *16*, 203-213.

- (10) Hoth, C. N.; Choulis, S. A.; Schilinsky, P.; Brabec, C. J. High Photovoltaic Performance of Inkjet Printed Polymer:Fullerene Blends. *Adv. Mater.* **2007**, *19*, 3973-3978.
- (11) Aernouts, T.; Aleksandrov, T.; Girotto, C.; Genoe, J.; Poortmans, J. Polymer Based Organic Solar Cells Using Ink-Jet Printed Active Layers. *Appl. Phys. Lett.* **2008**, *92*, 033306.
- (12) Jung, S.; Sou, A.; Banger, K.; Ko, D.-H.; Chow, P. C. Y.; McNeill, C. R.; Sirringhaus, H. All-Inkjet-Printed, All-Air-Processed Solar Cells. *Adv. Energy Mater.* **2014**, *4*, 1400432.
- (13) Xu, D.; Sanchez-Romaguera, V.; Barbosa, S.; Travis, W.; de Wit, J.; Swan, P.; Yeates, S. G. Inkjet Printing of Polymer Solutions and the Role of Chain Entanglement. *J. Mater. Chem.* **2007**, *17*, 4902-4907.
- (14) Hoath, S. D.; Harlen, O. G.; Hutchings, I. M. Jetting behavior of polymer solutions in drop-on-demand inkjet printing. *J. Rheol.* **2012**, *56*, 1109-1145.
- (15) Johns, A. S.; Bain, C. D. Ink-Jet Printing of High-Molecular-Weight Polymers in Oil-in-Water Emulsions. *ACS Appl. Mater. Interfaces* **2017**, *9*, 22918-22926.
- (16) van den Berg, A. M. J.; Smith, P. J.; Perelaer, J.; Schrof, W.; Koltzenburg, S.; Schubert, U. S. Inkjet Printing of Polyurethane Colloidal Suspensions. *Soft Matter* **2007**, *3*, 238-243.
- (17) Kuang, M.; Wang, J.; Bao, B.; Li, F.; Wang, L.; Jiang, L.; Song, Y. Inkjet Printing Patterned Photonic Crystal Domes for Wide Viewing-Angle Displays by Controlling the Sliding Three Phase Contact Line. *Adv. Opt. Mater.* **2014**, *2*, 34-38.
- (18) Wang, D.; Park, M.; Park, J.; Moon, J. Optical Properties of Single Droplet of Pphotonic Crystal Assembled by Ink-Jet Printing. *Appl. Phys. Lett.* **2005**, *86*, 241114.

- (19) Park, J.; Moon, J.; Shin, H.; Wang, D.; Park, M. Direct-write Fabrication of Colloidal Photonic Crystal Microarrays by Ink-Jet Printing. *J. Colloid Interface Sci.* **2006**, *298*, 713-719.
- (20) Cui, L.; Li, Y.; Wang, J.; Tian, E.; Zhang, X.; Zhang, Y.; Song, Y.; Jiang, L. Fabrication of Large-Area Patterned Photonic Crystals by Ink-jet Printing. *J. Mater. Chem.* **2009**, *19*, 5499-5502.
- (21) Deegan, R. D.; Bakajin, O.; Dupont, T. F.; Huber, G.; Nagel, S. R.; Witten, T. A. Capillary Flow as the Cause of Ring Stains from Dried Liquid Drops. *Nature* **1997**, *389*, 827-829.
- (22) Deegan, R. D.; Bakajin, O.; Dupont, T. F.; Huber, G.; Nagel, S. R.; Witten, T. A. Contact Line Deposits in an Evaporating Drop. *Phys. Rev. E* **2000**, *62*, 756-765.
- (23) Shen, X.; Ho, C.-M.; Wong, T.-S. Minimal Size of Coffee Ring Structure. *J. Phys. Chem. B* **2010**, *114*, 5269-5274.
- (24) Dou, R.; Wang, T.; Guo, Y.; Derby, B. Ink-Jet Printing of Zirconia: Coffee Staining and Line Stability. *J. Am. Ceram. Soc.* **2011**, *94*, 3787-3792.
- (25) Sun, J.; Bao, B.; He, M.; Zhou, H.; Song, Y. Recent Advances in Controlling the Depositing Morphologies of Inkjet Droplets. *ACS Appl. Mater. Interfaces* **2015**, *7*, 28086-28099.
- (26) Eral, H. B.; Augustine, D. M.; Duits, M. H. G.; Mugele, F. Suppressing the Coffee Stain Effect: How to Control Colloidal Self-Assembly in Evaporating Drops Using Electrowetting. *Soft Matter* **2011**, *7*, 4954-4958.
- (27) Kim, S. J.; Kang, K. H.; Lee, J.-G.; Kang, I. S.; Yoon, B. J. Control of Particle-Deposition Pattern in a Sessile Droplet by Using Radial Electroosmotic Flow. *Anal. Chem.* **2006**, *78*, 5192-5197.

- (28) Soltman, D.; Subramanian, V. Inkjet-Printed Line Morphologies and Temperature Control of the Coffee Ring Effect. *Langmuir* **2008**, *24*, 2224-2231.
- (29) Cui, L.; Zhang, J.; Zhang, X.; Huang, L.; Wang, Z.; Li, Y.; Gao, H.; Zhu, S.; Wang, T.; Yang, B. Suppression of the Coffee Ring Effect by Hydrosoluble Polymer Additives. *ACS Appl. Mater. Interfaces* **2012**, *4*, 2775-2780.
- (30) Kajiya, T.; Kobayashi, W.; Okuzono, T.; Doi, M. Controlling the Drying and Film Formation Processes of Polymer Solution Droplets with Addition of Small Amount of Surfactants. *J. Phys. Chem. B* **2009**, *113*, 15460-15466.
- (31) Park, J.; Moon, J. Control of Colloidal Particle Deposit Patterns within Picoliter Droplets Ejected by Ink-Jet Printing. *Langmuir* **2006**, *22*, 3506-3513.
- (32) Anyfantakis, M.; Baigl, D. Dynamic Photocontrol of the Coffee-Ring Effect with Optically Tunable Particle Stickiness. *Angew. Chem. Int. Ed.* **2014**, *53*, 14077-14081.
- (33) Talbot, E. L.; Yang, L.; Berson, A.; Bain, C. D. Control of the Particle Distribution in Inkjet Printing through an Evaporation-Driven Sol–Gel Transition. *ACS Appl. Mater. Interfaces* **2014**, *6*, 9572-9583.
- (34) Deng, R.; Liu, S.; Liang, F.; Wang, K.; Zhu, J.; Yang, Z. Polymeric Janus Particles with Hierarchical Structures. *Macromolecules* **2014**, *47*, 3701-3707.
- (35) Deng, R.; Li, H.; Liang, F.; Zhu, J.; Li, B.; Xie, X.; Yang, Z. Soft Colloidal Molecules with Tunable Geometry by 3D Confined Assembly of Block Copolymers. *Macromolecules* **2015**, *48*, 5855-5680.
- (36) Deng, R.; Li, H.; Zhu, J.; Li, B.; Liang, F.; Jia, F.; Qu, X.; Yang, Z. Janus Nanoparticles of Block Copolymers by Emulsion Solvent Evaporation Induced Assembly. *Macromolecules* **2016**, *49*, 1362-1368.

- (37) Weon, B. M.; Je, J. H. Capillary Force Repels Coffee-Ring Effect. *Phys. Rev. E* **2010**, *82*, 015305.
- (38) Harikrishnan, A. R.; Dhar, P.; Gedupudi, S.; Das, S. K. Effect of Interaction of Nanoparticles and Surfactants on the Spreading Dynamics of Sessile Droplets. *Langmuir* **2017**, *33*, 12180-12192.
- (39) Picknett, R. G.; Bexon, R. The Evaporation of Sessile or Pendant Drops in Still Air. *J. Colloid Interface Sci.* **1977**, *61*, 336-350.
- (40) Li, Y.-F.; Sheng, Y.-J.; Tsao, H.-K. Evaporation Stains: Suppressing the Coffee-Ring Effect by Contact Angle Hysteresis. *Langmuir* **2013**, *29*, 7802-7811.
- (41) Anyfantakis, M.; Baigl, D.; Binks, B. P. Evaporation of Drops Containing Silica Nanoparticles of Varying Hydrophobicities: Exploiting Particle–Particle Interactions for Additive-Free Tunable Deposit Morphology. *Langmuir* **2017**, *33*, 5025-5036.
- (42) Léopoldès, J.; Dupuis, A.; Bucknall, D. G.; Yeomans, J. M. Jetting Micron-Scale Droplets onto Chemically Heterogeneous Surfaces. *Langmuir* **2003**, *19*, 9818-9822.
- (43) Léopoldès, J.; Bucknall, D. G. Droplet Spreading on Microstriped Surfaces. *J. Phys. Chem. B* **2005**, *109*, 8973-8977.
- (44) Liang, R.; Wang, J.; Wu, X.; Dong, L.; Deng, R.; Wang, K.; Suen, M.; Liu, S.; Wu, M.; Tao, J.; Yang, X.; Zhu, J. Multifunctional Biodegradable Polymer Nanoparticles with Uniform Sizes: Generation and in Vitro Anti-melanoma Activity. *Nanotechnology* **2013**, *24*, 455302.
- (45) Pal, R. Phase Modulation Nanoscopy: A Simple Approach to Enhanced Optical Resolution. *Faraday Discuss.* **2015**, *177*, 507-515.

## Table of Contents

